Agricultural Water Management 164 (2016) 304–316

Contents lists available at ScienceDirect

Agricultural Water Management

journal homepage: www.elsevier.com/locate/agwat

Calibration of the AquaCrop model for winter wheat using MODIS LAI images

Andrea Trombetta[a,*], Vito Iacobellis[b], Eufemia Tarantino[b], Francesco Gentile[a]

[a] DISAAT Department, University of Bari, Via Amendola 165/A, Italy
[b] DICA TECH Department, Politecnico di Bari, Via Orabona 4, Italy

ARTICLE INFO

Article history:
Received 7 May 2015
Received in revised form 19 September 2015
Accepted 14 October 2015
Available online 2 November 2015

Keywords:
AquaCrop
Canopy cover
LAI
MODIS images
Model assessment

ABSTRACT

In semi-arid environments vegetation density and distribution is of considerable importance for the hydrological water balance. A number of hydrological models exploit Leaf Area Index (LAI) maps retrieved by remote sensing as a measure of the vegetation cover, in order to enhance the evaluation of evapotranspiration and interception losses.

On the other hand, actual evapotranspiration and vegetation development can be derived through crop growth models, such as AquaCrop, developed by FAO (Food and Agricultural Organization), which allows the simulation of the canopy development of the main field crops. We used MODIS LAI images to calibrate AquaCrop according to the canopy cover development of winter wheat. With this aim we exploited an empirical relationship between LAI and canopy cover. In detail Aquacrop was calibrated with MODIS LAI maps collected between 2008 and 2011, and validated with reference to MODIS LAI maps of 2013–2014 in Rocchetta Sant'Antonio and Sant'Agata, two test sites in the Carapelle watershed, Southern Italy. Results, in terms of evaluation of canopy cover, provided improvements. For example, for Rocchetta Sant'Antonio, the statistical indexes varyfrom $r = 0.40$, ER = 0.22, RMSE = 17.28 and KGE = 0.31 (using the model without calibration), to r = 0.86, ER = 0.08, RMSE = 6.01 and KGE 0.85 (after calibration).

1. Introduction

Hydrological processes within the Mediterranean area are highly variable both in space and time due to rainy regime, topography, soil conditions and land use (Moussa et al., 2007). In this context, hydrologic distributed models play a key role due to the increasing use of physical information provided by remote sensed data (e.g., Iacobellis et al., 2013). Particularly variables that quantify the development of vegetation cover are useful to estimate evapotranspiration and interception losses as well as in the assessment of soil erosion (van der Knijff et al., 2000; Kamaludin et al., 2013).

In this field, the use of crop growth models is crucial in order to optimize agricultural practices and, even more important, in order to model the vegetal cover variations at a yearly scale. Nevertheless their use at regional scale is limited by the need of intensive ground-based datasets that are necessary for calibration and testing. Among many growth models available in literature, that present a large number of variables not easily to compute (Raes et al., 2012), in this study we used the FAO AquaCrop model. With its reduced number of parameters AquaCrop is characterized by a better balance between simplicity, accuracy and robustness, than other crop models (Steduto et al., 2008). AquaCrop has been extensively tested across different regions in the world and different crops (e.g., Ahmadi et al., 2015). Nevertheless, without specific calibration of main parameters it still shows large uncertainties in the evaluation of important outputs such as actual evapotranspiration, soil moisture and crop yield. In this work we try to enhance the use of AquaCrop at regional scale exploiting the availability of a well established remote sensing product such as the MODIS-LAI images.

Remote or proximal sensing techniques that use spectral approaches can provide a rapid identification of water stress through many vegetation indices (Rinaldi et al., 2015). Particularly, Leaf Area Index (LAI) and canopy cover (CC) assume considerable relevance in the definition of crop development models and ecological processes analysis (Griffin et.al., 2008).

LAI is a dimensionless variable defined as the ratio between the total leaf surface and the leaf surface projected on the ground (Ross, 1981). This dynamic index is related to photosynthesis, transpiration surface of forest cover (Jonckheere et al., 2004), rainfall interception and energy exchange between vegetation and the atmosphere (Leuschner et al., 2006). Accordingly, LAI was also implemented in hydrological modelling, e.g., DREAM model

* Corresponding author.
E-mail address: andrea.trombetta@outlook.com (A. Trombetta).

http://dx.doi.org/10.1016/j.agwat.2015.10.013
0378-3774/

(Manfreda et al., 2005). Remote sensing provides the only reliable option for mapping LAI continuously over the globe (Tarantino et al., 2015a,b). LAI retrieval from passive remotely sensed data has been evaluated through semi empirical-statistical approach or with radiative transfer model (RTM) inversion of leaf canopy reflected energy (Zheng and Moskal, 2009). In the first mentioned approach LAI is estimated through vegetation indices (e.g., Clevers, 1989; Rouse et al., 1974; Stenberg et al., 2004) while the second one require an inversion of physical based models (e.g., Darvishzadeh et al., 2008; Fei et al., 2012; Houborg et al., 2015).

In this study LAI maps derived from the Moderate Resolution Imaging Spectroradiometer (MODIS), particularly the MCD15A2 level-4 product were used. The MODIS instrument was designed and developed following the science community objective to collect high temporal resolution global data useful for short/long term environmental studies (Xiong and Barnes, 2006). Modis is part of the payload of the National Aeronautics and Space Administration (NASA) Terra and Aqua satellites respectively known also as Earth Observation System (EOS) AM-1 and EOS PM-1. The MCD15A2 level-4 product is available at 1 km spatial resolution and at time-steps of 8–16 days. The algorithm implements a land cover classification where six biome types (respectively grasslands and cereals, shrubs, arable broadleaf, wooded meadows, broadleaf forest and coniferous woodland) are distinguished (Altobelli et al., 2007). Each biome represents a pattern of the architecture of an individual tree and the entire canopy as well as patterns of spectral reflectance and transmittance of vegetation elements (Knyazikhin et al., 1998; Weiss et al., 2000).

CC is defined as the ground fraction covered by the vertical projection of the trees (Nilson and Kuusk, 2004), and is commonly expressed in percentage terms (canopy cover percentage, or its inverse, canopy openness percentage). CC is a parameter useful in forest ecology and is used to study the potential risk of fire, watershed, erosion and illegal logging (Chopping et al., 2008; Ozdemir, 2014). Both the United Nation of Food and Agriculture (FAO) and the National Land Cover Database (NLCD) used CC to identify tree covered areas (FAO, 2010; Homer et al., 2007).

LAI and CC are estimated also by growth models. Particularly interesting is the integration of remote sensing data into crop growth models with the aim of improving the accuracy of model simulation (Dente et al., 2008; Huang et al., 2015; Jongschaap, 2006; Mo et al., 2005). Maas (1993) compared the results of calibrating a crop simulation model on winter wheat using LAI observation from field and remote sensing. Moulin et al. (1998) in a review paper described the relations between crop state variables and satellite observations. Weiss et al. (2001) described the process of coupling the STICS model (Brisson et al., 1998) with the SAIL RTM (Verhoef, 1984) and then performed a sensitivity analysis to select crop model parameters that mostly influenced the radiometric signal. Bach et al. (2001) combined the PROMET-V (Schneider and Mauser, 2001) and the SAIL with good results in the estimation of LAI, canopy ehight and dry biomass. Doraiswamy et al., (2004) investigasted the usefulness of MODIS data both to assess crop condition and in crop simulation model. LAI maps derived both from active and passive sensor were assimilated in Dente et al. (2008) in order to improve the wheat yield prediction accuracy using the CERES–Wheat model. Fang et al., 2008 developed a procedure to predict regional crop yield estimation from MODIS data. Xu et al., 2011 implemeted the phenology information derived from the MODIS LAI product in the SWAP model (Van Dam et al., 1997) for winter wheat estimation at regional scale. The MODIS LAI product was also used by Fang et al., 2011 to estimate the corn yeld with the CSM–CERES–Maize model model coupled with the MCRM model (Kuusk, 1998). Huang et al., 2015 implemented whithin the WOFOST model LAI derived from MODIS and LANDSAT™ data to predict winter wheat yield at regional scale.

Table 1
Main characteristics of the Carapelle watershed.

Watershed area	982.6 km^2
Maximum altitude	1075 m a.s.l
Average altitude	540 m a.s.l.
Mean watershed slope	4.4%
Mean annual rainfall (Rocchetta Sant'Antonio)	1.94 mm
Mean annual rainfall (Sant'Agata di Puglia)	2.00 mm
Mean annual temperature (Rocchetta Sant'Antonio)	13.67 °C
Mean annual temperature (Sant'Agata di Puglia)	13.84 °C

The aim of this paper is to assess the AquaCrop model performances by exploiting the LAI–CC variability of winter durum wheat, which is the predominant type of vegetation in a study area within the Carapelle's catchment, in Southern Italy, using the MODIS images for model calibration and validation. For this purpose, the LAI–CC empirical relationship found by Nielsen et al. (2012) was used.

Calibration and validation were carried out separately using MODIS low-resolution images: the calibration was developed in 2009–2010 in Rocchetta and between 2008 and 2010 in Sant'Agata, while the validation was carried out in 2013–2014 for both sites.

2. Materials and methods

2.1. Study area

The test sites are close to the towns of Rocchetta Sant'Antonio and Sant'Agata di Puglia respectively, both in the Carapelle riverbasin. Furthermore the Lacedonia weather station, located close to the previous ones, was considered in case of missing data. The main stream of Carapelle originates in the Campanian Apennine, from La Forma Mountain, and flows into the Adriatic Sea. The catchment has a watershed area of 982.6 km^2 (Table 1, Figs. 1 and 2).

The river regime is torrential, with streamflow generally high in November and December, dry in July and August. The climate is typically Mediterranean with moderately rainy winters, warm and dry summers. The rainfall range is from 477 to 815 mm/year and the average temperatures range from 10 to 16 °C/year. The main cultivations are durum wheat (85% of total basin area), different types of vegetables and olives groves, localized in low hilly and plain areas, while forests and pasture are present in the higher slopes (Milella et al., 2012). The size of the two study sites is approximately 1 km^2 (Fig. 2).

2.2. Model description

AquaCrop (http://www.fao.org/nr/water/aquacrop.html) is a software system developed by the Land and Water Division of FAO in order to increase water efficiency practices in agricultural production (Araya et al., 2010). AquaCrop uses the first Doorenbos and Kassam (1979) equation for the biomass calculation and, finally, the crop yield, proportional to the biomass according to a "harvestable part". The software simulates Biomass (B) and Yields (Y) production of agricultural crops, focusing on water stress conditions (Steduto et al., 2009). The model is based on the water resource used in transpiration, which results in biomass using a crop-specific conservative parameter (Geerts et al., 2009).

The stress coefficients play a key role in the model. They describe the different stress conditions, detected in the crop biomass production (wheat, vegetables). These coefficients "continuously adjust" the computed quantities in each calculation step. They vary between 1 (no stress) and 0 (max stress) (Fig. 3).

The stress coefficients account for soil water, air temperature, soil fertility and salinity. They affect the canopy expansion pro-

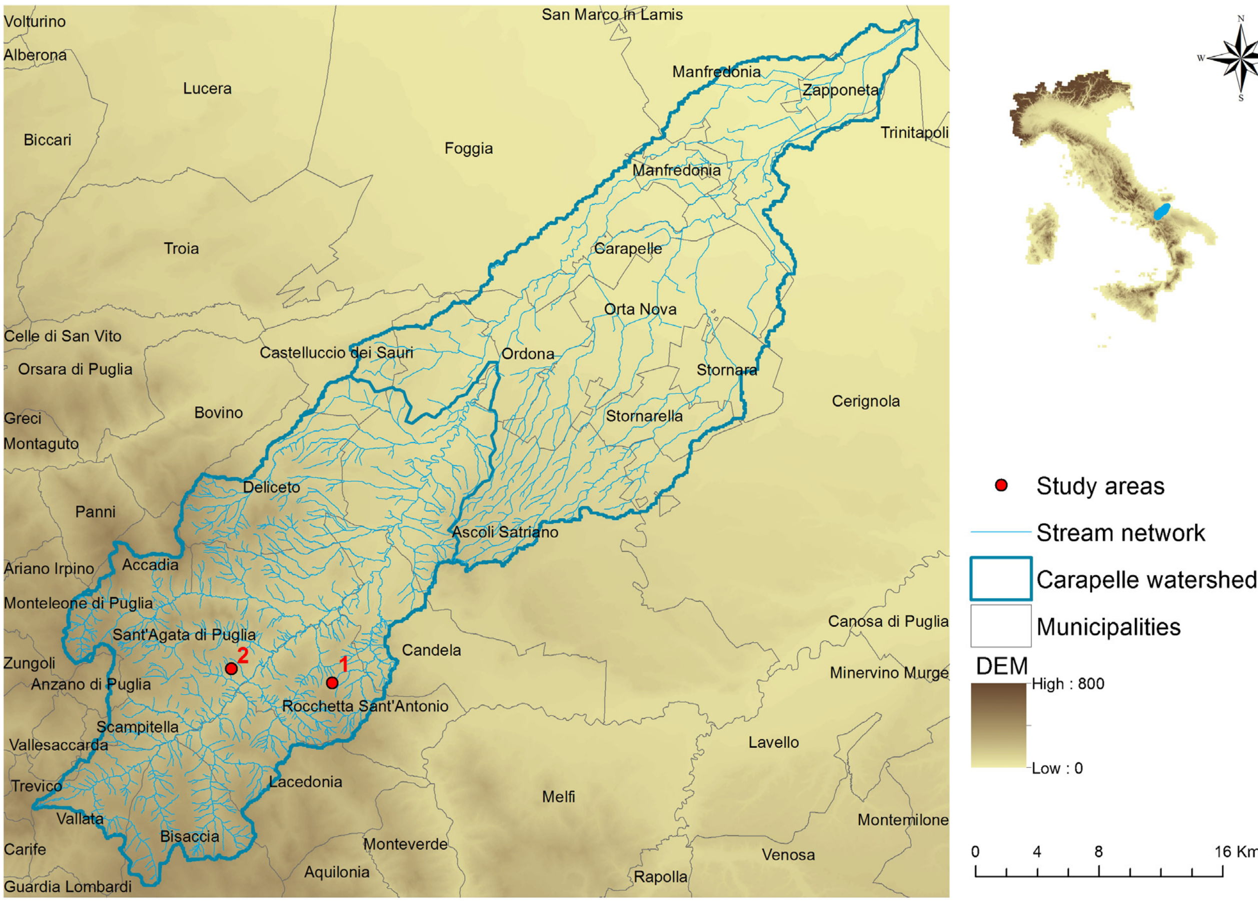

Fig. 1. Study area: the Carapelle watershed.

cesses, stomata control of transpiration, canopy senescence and Harvest Index HI.

The soil water balance, the green canopy cover, the crop transpiration, the above ground Biomass and Yield form the software calculation scheme. In the calculation scheme, different parameters operate among the variables above: crop coefficient (kc), water productivity (WP) and, finally, Harvest Index (HI). Among these parameters HI plays a key role by partitioning Biomass (B) into Yield (Y). HI grows up linearly in time after a lag phase, up to physiological maturity (Raes et al., 2012).

The canopy cover is a crucial feature in AquaCrop, because through its expansion, ageing, conductance and senescence, it determines the amount of water transpired (T_r), which in turns determines the amount of Biomass produced (B) and the final Yield (Y) (Raes et al., 2012).

Reference evapotranspiration is preliminarily evaluated to calculate transpiration using the FAO ET_0 calculator. The Penman–Monteith formula is used (Eq. (1)):

$$ET_0 = \frac{0.408\Delta\,(R_n - G) + \gamma\frac{900}{T+273}u_2\,(e_s - e_a)}{\Delta + \gamma\,(1 + 0.34u_2)} \qquad 1$$

where ET_0 is the reference evapotranspiration [mm day^{-1}], R_n net radiation at the crop surface [MJ m^{-2} day^{-1}], G soil heat flux density [MJ m^{-2} day^{-1}], T mean daily air temperature at 2 m height [°C], u_2 wind speed at 2 m height [m s^{-1}], e_s saturation vapour pressure [kPa], e_a actual vapour pressure [kPa], e_s–e_a saturation vapour pressure deficit [kPa], D slope vapour pressure curve [kPa °C^{-1}], γ psychrometric constant [kPa °C^{-1}]. ET_0 is related to the actual vegetation cover through the crop coefficient kc, which depends on crop type, sowing or planting period, duration of crop development stages and growing period under prevailing climatic conditions (Semaika and Rady, 1987).

The software comprises four separate workplaces: Environment and Crop, Simulation, Project, Field Data. The data are contained in specific files, including climate, crop, soil and management (irrigation), initial soil water condition (Raes et al., 2009). The basic measurement unit for simulations follows a thermal approach in °C at temporal daily scale, the GDD (Growing Degree Days).

AquaCrop uses a relatively small number of explicit and very intuitive parameters trying to balance simplicity, accuracy and robustness (Andarzian et al., 2011). Raes et al. (2009) describe the software operation in detail. Moreover a complete model description is provided by Steduto et al. (2009).

2.3. Data acquisition

The Aquacrop crop growth software requires detailed physical, land use and climate data. GeoEye high-resolution (2 m) (Aquilino et al., 2014) and MODIS low resolution (1 km) remote sensing data were used to calibrate and validate the model.

The climate inputs are rainfall, air temperature and wind speed. Time series of rainfall, temperature and wind speed, recorded by the Civil Protection Agency of Regione Puglia, are available. For this study, daily data on rainfall, minimum and maximum temperature from Sant'Agata and Rocchetta stations, and mean daily wind speed from anemometric Biccari station were used. The use of thermometer and rain gauge stations was assessed by using the Thiessen weighting procedure.

In case of missing data, regression formulas between the main station of Rocchetta and that of Lacedonia, located very close one

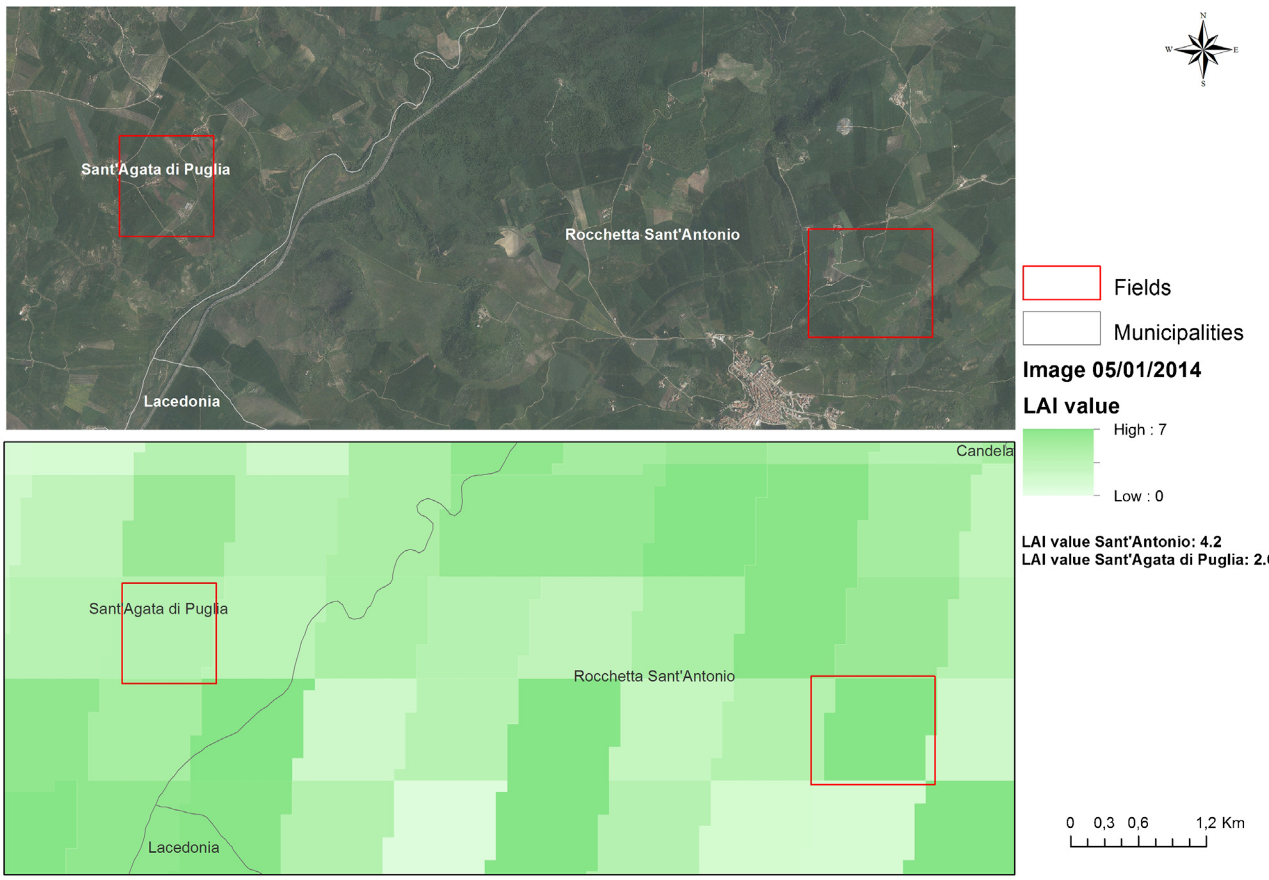

Fig. 2. Position of two work field and LAI-MODIS image of 05/01/2014.

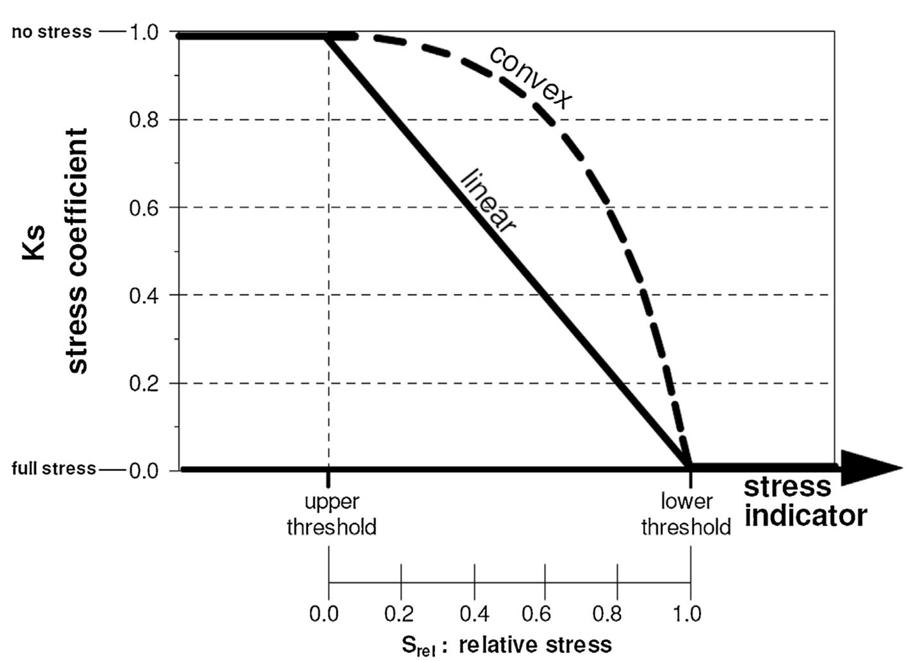

Fig. 3. The stress coefficient (*Ks*) for various degrees of stress and for different shapes of the *Ks* curve (Raes et al., 2012).

to the other, were used. The results showed a strong correlation in terms of rainfall and minimum and maximum temperature of the two sites (Fig. 4a–c). Good correlation exists also between Sant'Agata and Lacedonia for rainfall (Fig. 4d).

The reference evapotranspiration was estimated by the Penman–Monteith equation, which requires the measures of temperature, humidity of air, solar radiation and wind speed. These climatic quantities, not directly available, were derived from temperature and wind speed, as described in Allen et al.(1998) .

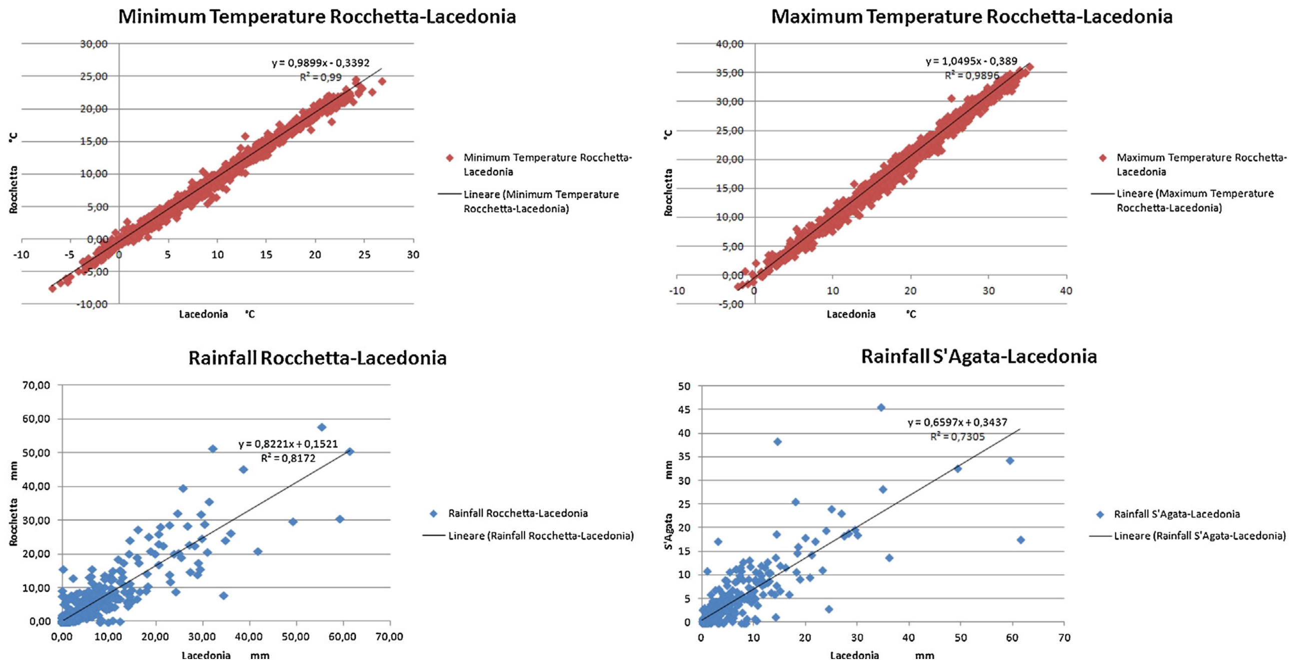

Fig. 4. Rocchetta-Lacedonia (a–c), Sant'Agata-Lacedonia regression (d).

Land use and vegetal coverage were obtained from the Puglia Information System SIT, at the website http://www.sit.puglia.it/portal/portale_cartografie_tecniche_tematiche/Download/Cartografie, at 1:5000 scale.

Soil parameters such as the textural classes, saturated hydraulic conductivity, soil depths and porosity were extracted from the ACLA2 project (scale 1:100,000), a research program funded by the Puglia region and aimed at agro-ecological characterization of the region on the basis of laboratory tests, field observation and photo interpretation of aerial photograph and satellite images (Caliandro et al., 2005).

The texture classes were found using the USDA textural triangle. The hydraulic soil properties (the volumetric soil moisture contents at saturation (θ_{max}), wilting point (θ_{wp}) and field capacity (θ_{FC}), hydraulic conductivity at saturation (k_s)) were estimated using the Saxton and Rawls (Saxton et al., 1986; Saxton and Rawls, 2006) pedotransfer functions, which are implemented in a calculator at the website http://hrsl.ba.ars.usda.gov/soilwater/Index.htm. The second level Saxton and Rawls algorithm (according to the classification of Ungaro and Calzolari, 2001) starts from clay (C) and sand (S) weight percentages, and from organic matter (OM), which is related to organic carbon content (OC) when direct measurements are not available. These quantities are freely available on the website http://eusoils.jrc.ec.europa.eu/ESDB_Archive/octop/octop_data.html, at a resolution of 1 km.

TheorganicmatterisrelatedtoorganiccarbonwithEq.(2)

$$OM = OC \times 1.724 \quad (2)$$

The MODIS images (MODerate resolution Imaging Spectroradiometer) are freely available on the NASA website (https://lpdaac.usgs.gov/products/modis_products_table). The MODIS images (hdf-eos format) are processed by the reprojection MODIS tool, freely available on the USGS EROS Data Center website (https://lpdaac.usgs.gov/tools/modis_reprojection_tool).

High-resolution GeoEye images were acquired for the 13/05/2009 scene in Sant'Agata and for the 29/04/2010 scene for both Rocchetta and Sant'Agata. Previous studies demonstrated the compatibility of LAI retrieved though very high spatial resolution satellite data with MODIS LAI data (Aquilino et al., 2014; Tarantino et al., 2015a,b).

2.4. LAI–canopy cover relationships

The Leaf Area Index (LAI) and the canopy cover percentage are two expressions of the vegetation cover and become relevant in the crop development models and the ecological processes analysis (Griffin et al., 2008).

LAI is a positive variable and its values depend on several factors, such as climate, water availability and development stages. A LAI value equal to zero represents the bare soil, while high values account for a dense vegetation cover.

LAI values are obtained by MODIS and GeoEye images while AquaCrop evaluates the Green Canopy Cover.

For this reason, a relationship between these two variables which depend onthe crop/vegetation types,the water supply type (irrigation or not), the crop density and the management practices, the seasonal and inter-annual variability, is needed.

Many authors proposed several conversion equations for specific crop/vegetation and relative canopy architecture, (Buckley et al., 1999; Wang et al., 2005; Hsiao et al., 2009; Nielsen et al., 2012)

In this study, the empirical relationship Eq. (3) proposed by Nielsen et al., (2012) was applied as it is referred to a winter wheat crop:

$$CC = 94.00 \times [1 - \exp(-0.43 \times LAI)]^{0.52} \quad (3)$$

with $R^2 = 0.957$.

2.5. Calibration/validation process

Any model should be carefully parameterized, calibrated and validated before its practical use (Addiscott et al., 1995; Nain and Kerebaum, 2007; Biondi et al., 2012). During parameterization and calibration, the model's parameters and even the code may be changed in order to obtain accurate simulated values versus the observed data. In contrast, during validation, the model is run without any modification of the model's parameters or code, which is compared to independent experimental data (Nain and Kersebaum, 2007; Salazar et al., 2009).

AquaCrop is designed to be widely applied under different climatic and soil conditions, without particular crop parameterizations (Hsiao et al., 2012). The parameters used in the model are subdivided into conservative parameters, constant according to the boundary conditions, and parameters based on location, crop cultivars and management practices. However many of the conservative parameters are obtained from modern high-yielding cultivars grown with optimal soil fertility without limitations from any mineral nutrient, particularly nitrogen (Hsiao et al., 2012). Moreover, there are also parameters of cultivar-specific type, i.e., parameters similar to the conservative ones, which present slight variations within the same crop species, due to different cultivar classes. During calibration the available calibrated parameters are used as a starting point and are adjusted by means of local measurements.

The canopy cover time series is used to calibrate the model. By its expansion, development and senescence, the transpired water quantity is obtained, which subsequently determines the Biomass production.

Hence the simulated CCs are compared to the corresponding observed values. The parameters affecting the CC development are: plant density, initial canopy cover (CCo), time from sowing to emergence, time from sowing to senescence, time from sowing to maturity, maximum canopy cover (CCx), canopy growth coefficient (CGC), canopy decline coefficient (CDC) and maximum effective rooting depth (Z*x*).

Canopy development is simulated by two equations:

Eq. (1) (exponential growth) is valid when $CC \le CC_x/2$

$$CC = CC_0 e^{tCGC} \tag{4}$$

Eq. (2) (exponential decay) is valid when $CC > CCx/2$

$$CC = CC_x - 0.25\frac{(CC_x)^2}{CC_0}e^{-tCGC} \tag{5}$$

where *t* is the time, (Raes et al., 2012).

We started from the parameter values available in scientific literature about the wheat grown in the Carapelle basin to determine the phenological phases, while with regard to the other parameters the default values of the crop calibrated within the software were used as the starting point. The calibration was carried out following a trial and error technique, varying the calibration parameters and evaluating the differences between simulation and MODIS-observation data.

The soil water content at the beginning of the simulation was chosen as the minimum value reached after the summer dry season and was assumed to be equal to the permanent wilting point, PWP.

2.6. Performance metrics

We used several statistical indices for model calibration and validation, such as the root mean square error (RMSE), relative error (ER), linear correlation coefficient (*r*), relative variability, relative bias and Kling–Gupta Efficiency (KGE).

The root mean square error is given by Eq. (6):

$$RMSE = \sqrt{\frac{\sum (P_i - O_i)^2}{n}} \tag{6}$$

where O_i and P_i are the observed and predicted values (MODIS measures and simulated respectively), and n the number of observations. A disadvantage of RMSE lies in that the residual errors are calculated as squared values, which means that higher values in a time series are given greater weight than lower values (Legates and McCabe, 1999).

The relative error (ER%) (Eq. (7)):

$$ER = \frac{P_i - O_i}{O_i} \tag{7}$$

Gupta et al. (2009) highlighted some critical points related to the performance metrics most used in hydrology, i.e., the NSE and RMSE. They showed that NSE (Nash and Sutcliffe, 1970) can be broken down into three distinctive components and namely: the linear correlation (*r*) between simulations and observations, the bias normalized by the standard deviation in the observed values and a measure of relative variability in the simulated and observed values (α). Gupta et al. (2009) proposed the Kling–Gupta efficiency defined as (8, 9, 10):

$$\alpha = \frac{\sigma_s}{\sigma_o} \tag{8}$$

$$\beta = \frac{\mu_s}{\mu_o} \tag{9}$$

$$KGE = 1 - \sqrt{(r-1)^2 + (\alpha-1)^2 + (\beta-1)^2} \tag{10}$$

where σ is the standard deviation and μ is the mean value (with subscript "s" for simulations and "o" for observations), α is the relative variability and β is the relative bias.

3. Results and discussion

3.1. Calibration

In the Table 2 the the soil properties and the hydraulic soil propertiesused to run the model are reported for Rocchetta Sant'Antonio and Sant'Agata di Puglia.

In Table 3 the values assigned to specific model parameters are reported both for Rocchetta Sant'Antonio and Sant'Agata di Puglia. Fig. 5 shows the CC values simulated by Aquacrop after calibration and those obtained from the MODIS images in 2009–2010 where the model simulates accurately the CC behavior.

The calibration of Sant'Agata was more accurate inasmuch as there are two years of observations. Moreover, in 2008–2009 the CC values are lower than in 2009–2010 as shown in Figs. 6 and 7, where both the CC simulated values and those obtained from the MODIS images are reported. In the same figures the data obtained from the high resolution GeoEye sensor data are reported. These images refer to April 29 2010 both for Rocchetta and Sant'Agata and to May 13 2009 for Sant'Agata. The model seems to provide an almost systematic overestimation in 2008–2009 simulations and is more in line for the years 2009–2010.

In the entire investigation period, the average CC values of Rocchetta were found to be higher than those in Sant'Agata, probably due to the different topographical exposure conditions of the two sites.

A good fit was observed in all the simulations, but after the flowering stage we noticed that senescence was slightly faster compared to simulations, in agreement with the comments by Andarzian et al., 2011. The reason for this behavior may be due to the effect of high-temperature stress on CC, which is not considered in the model (Andarzian et al.,2011).

The statistical indices are reported in Table 4:

The production of Biomass (B) and Yield (Y) seems overestimated with respect to the amounts usually obtained in these areas (Table 5), which, according to local producers, range between 3.5 and 5 ton/ha (Quaranta et al., 2015).

Statistical indexes are good in all simulations, particularly for Sant'Agata 2009–2010, in which all the efficiency indices achieve excellent values, as for example, RMSE which achieves the average value of 9% (Table 4 and Figs. 8–10). In Figs. 8–10 the relative error

Table 2
Soil properities of Rocchetta Sant'Antonio and Sant'Agata di Puglia.

Soil properties Rocchetta Sant'Antonio									
Layers number	Soil type	Texture classes (USDA triangle)		Organic content (OC)	Organic matter (OM)	Hydraulic soil properties			
		%				θ_{SAT} (%)	θ_{WP} (%)	θ_{FC} (%)	k_S (mm/h)
1	LOAM	Sand	42	1.702482	2.93507	46.9	12.9	27.2	20.33
		Clay	18						
		Silt	40						
Soil properties Sant'Agata di Puglia									
Layers number	Soil type	Texture classes (USDA triangle)		Organic content (OC)	Organic Matter (OM)	Hydraulic soil properties			
		%				θ_{SAT} (%)	θ_{WP} (%)	θ_{FC} (%)	k_S (mm/h)
1	LOAM	Sand	42	1.635032	2.818795	46.6	12.8	27.0	19.89
		Clay	18						
		Silt	40						

Table 3
Values assigned to specific model parameters to simulate the responses of winter wheat in Rocchetta Sant'Antonio and Sant'Agata di Puglia. L means that the value has been taken as default or from literature; C if it comes from calibration.

Parameter description	Range suggested by the model	Rocchetta input values	Sant'Agata input values	Unit or meaning	
Time from sowing to emergence	100–250	224	224	GDD	C
Time from sowing to maximum canopy cover	derived	1124	1119	GDD	/
Time from sowing to start of canopy senescence	Time to emergence + 1000–2000	1244	1201	GDD	C
Time from sowing to maturity	Time to emergence + 1500–2900	2309	2399	GDD	C
Time from sowing to flowering	Time to emergence + 900–1300	1024	1149	GDD	C
Duration of flowering	150–280	285	267	GDD	C
Canopy size seedling	1.50	1.50	1.50	cm^2/plant, the area of initial plant	L
Maximum canopy cover (CCx)	80–99%	90%	79	The maximum permissible canopy cover	C
Canopy growth coefficient (CGC)	0.5–0.7	0.613	0.602	%/GDD the maximum permissible increase of CC	C
Canopy decline coefficient (CDC)	0.4	0.247	0.191	%/GDD the maximum permissible decrease of CC	C
Maximum effective rooting depth (Zx)	Up to 2.40	1.5	1.5	m	L
Time from sowing to maximum rooting depth	derived	725	725	GDD	/
Base temperature	0.0	0.0	0.0	°C, Crop growth stops below this temperature	L
Upper temperature	26.0	26.0	26.0	°C, Crop growth stops above this temperature	L
Crop coefficient for transpiration (kc_{Tr})	1.10	1.10	1.10	Full canopy transpiration relative to ETo	L
Water productivity (WP)	15.0	15.0	15	g(biomass)/m^2, function of atmospheric CO_2	L
Reference harvest index (HIo)	45-50%	43%	43	The harvest index under optimal conditions	C
Length building up HI	derived	1262	1181	GDD, the period during which the yield increase	/

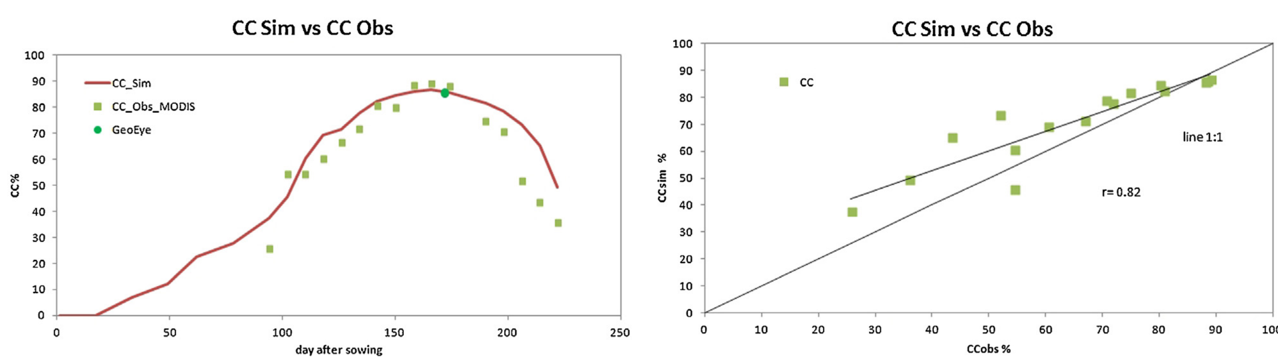

Fig. 5. Simulated and Observed CC of winter wheat in Rocchetta Sant'Antonio 2009–2010.

referred to each MODIS image is reported, while Table 4 shows the mean relative error referred to all the simulation.

3.2. Validation

The validation step was carried out with reference to the period 2013–2014. In order to assess the improvements made through the previous calibration phase, the model results were compared with those obtained with model runs in which default values for the winter wheat in AquaCrop were used. The simulation runs with default values for Rocchetta are indicated with ValenzanoP1 while those for Sant'Agata with ValenzanoP2. The results are shown in Figs. 11 and 12.

By analyzing time series graphics and statistical indices (Table 4) we observe that significant improvements are provided by calibration in both sites. The relative error decreases from 0.22 to 0.08

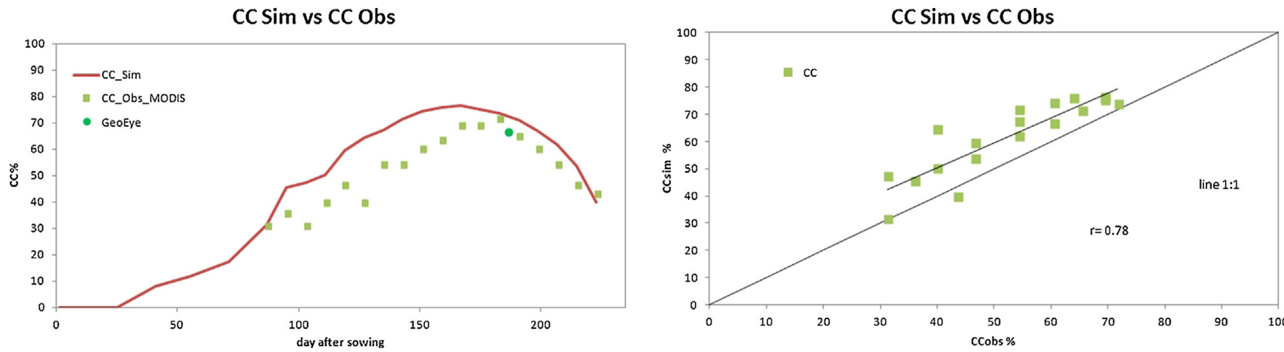

Fig. 6. Simulated and Observed CC of winter wheat in Sant'Agata di Puglia 2008–2009.

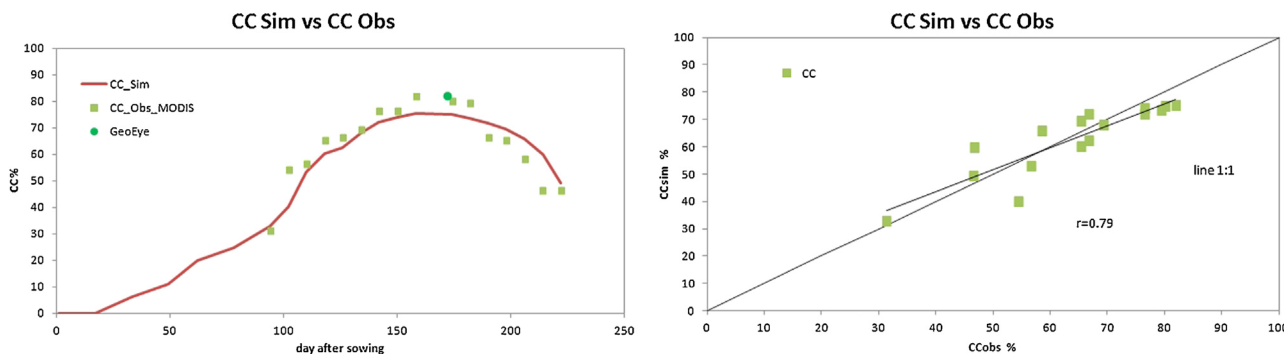

Fig. 7. Simulated and Observed CC of winter wheat in Sant'Agata di Puglia 2009–2010.

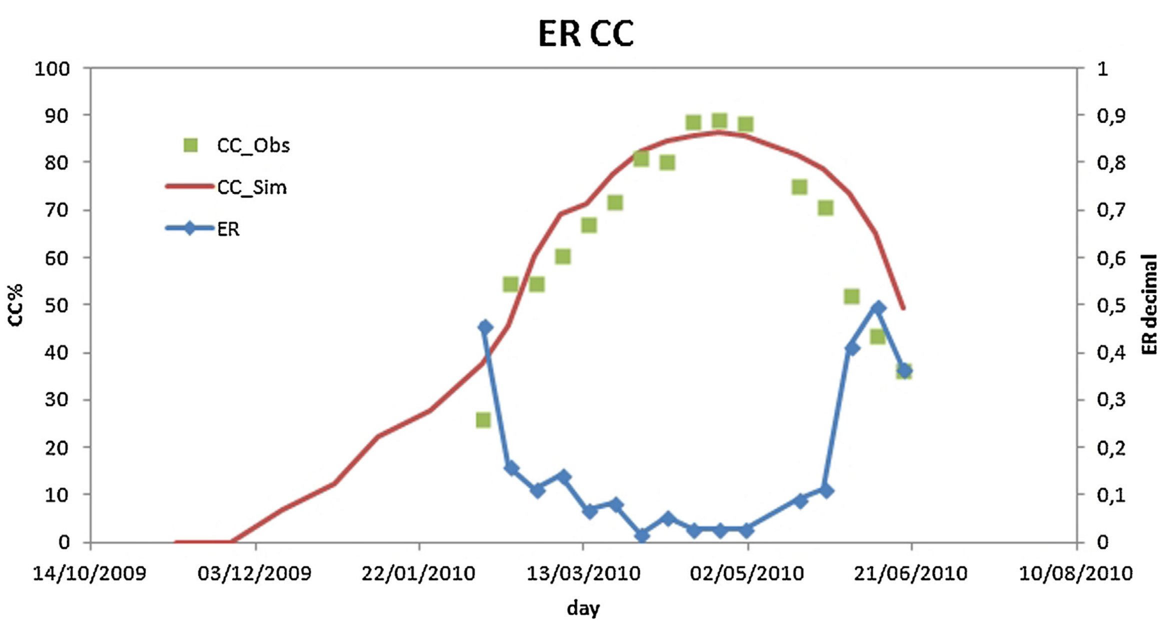

Fig. 8. Relative error in calibration Rocchetta Sant'Antonio 2009–2010.

for Rocchetta and from 0.38 30 to 0. 19 for Sant'Agata. The RMSE also shows a decrement from 17.28 to 6.01 for Rocchetta, and from 30.29 to 12.27 for Sant'Agata. A better performance was noticed even when looking at α and β values.

When observing the relative error time series, average improvements of about 20% are recorded for both study sites (Fig. 13(a), and (b).

The default winter wheat within AquaCrop leads to an overestimation of the CC performance (Fig. 13(c) and (d) in agreement with Hsiao et al., 2012.

Finally, Biomass and Yield (Table 5) show lower values using calibration than the default AquaCrop cultivation, so they are closer to the quantities obtained for the 2014 yield, which is approximately 4.5 ton/ha based on information collected in the areas under study and according to what reported by Quaranta et al. (2015). Also in this case the highest yields are due to the Hsiao et al., 2012 condi-

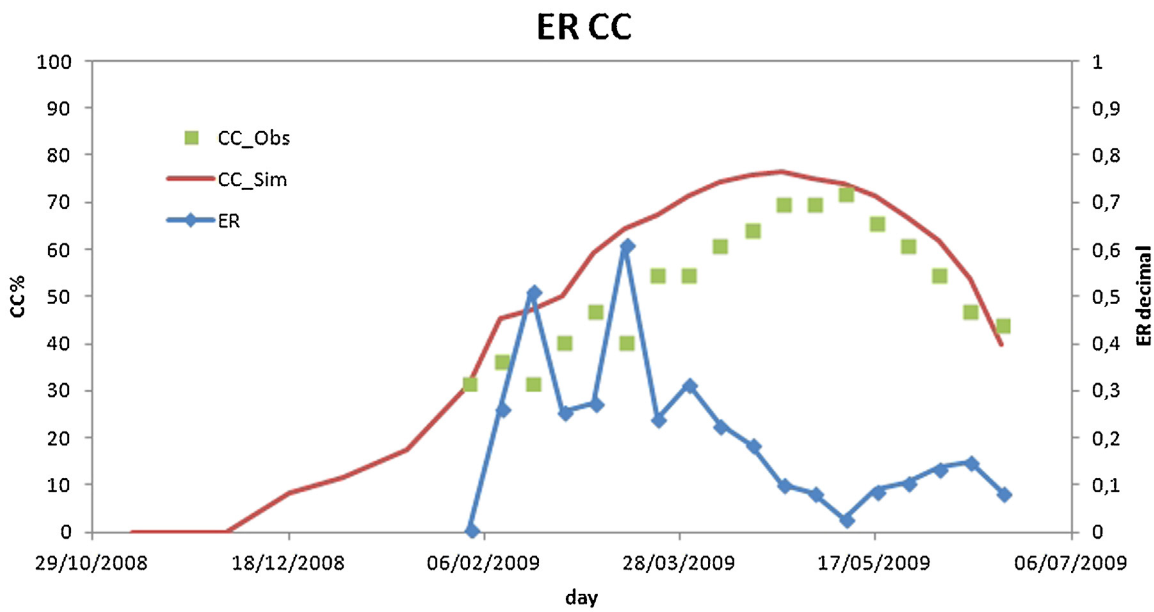

Fig. 9. Relative error in calibration Sant'Agata di Puglia 2008–2009.

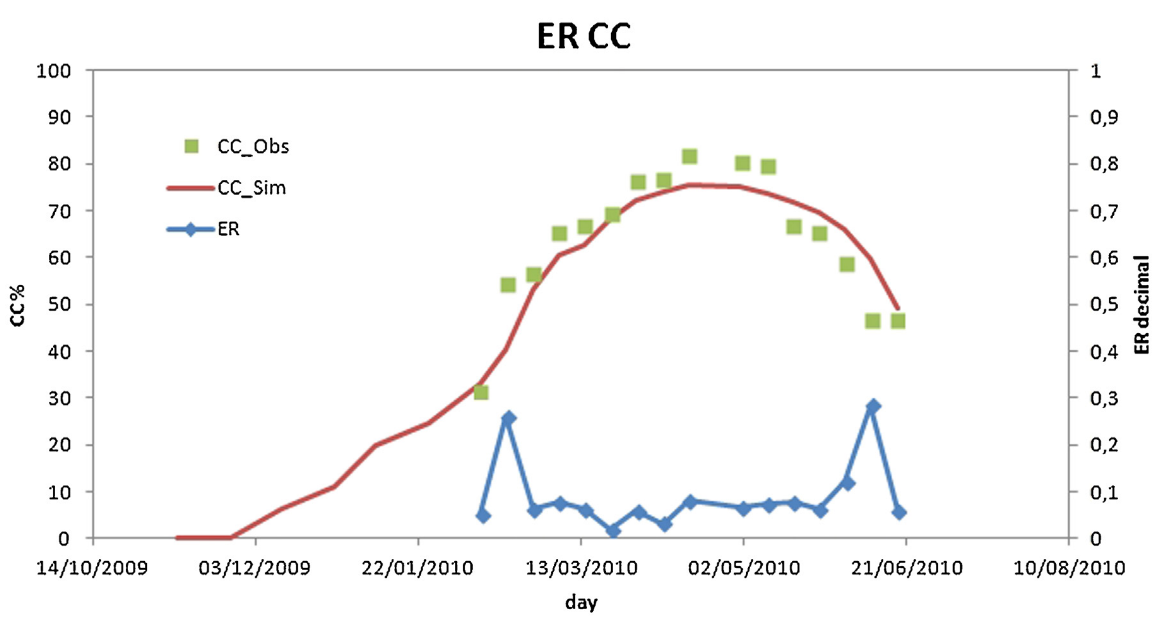

Fig. 10. Relative error in calibration Sant'Agata di Puglia 2009–2010.

Table 4
Statistical parameters of calibrated and validated points.

	RMSE CC	ER CC	α CC	β CC	r CC	KGE CC
Calibration						
Rocchetta 2009–2010	10.11	0.17	0.82	1.08	0.90	0.77
Sant'Agata 2008–2009	11.26	0.20	1.03	1.18	0.88	0.78
Sant'Agata 2009–2010	6.48	0.09	1.20	0.95	0.88	0.86
Validation						
Rocchetta 2013–2014	6.01	0.08	0.94	1.03	0.86	0.85
ValenzanoP1 2013–2014	17.28	0.22	0.71	1.19	0.40	0.31
Sant'Agata 2013–2014	12.27	0.19	1.07	1.02	0.58	0.57
ValenzanoP2 2013–2014	30.29	0.38	1.01	1.35	0.80	0.56

Table 5
Biomass and yield of calibrated and validated points.

	Biomass	Yield
	ton/ha	ton/ha
Calibration		
Rocchetta 2009–2010	14.683	6.314
Sant'Agata 2008–2009	13.173	5.664
Sant'Agata 2009–2010	13.444	5.719
Validation		
Rocchetta 2013–2014	15.460	6.486
ValenzanoP1 2013–2014	19.036	9.139
Sant'Agata 2013–2014	14.704	6.321
ValenzanoP2 2013–2014	18.244	8.601

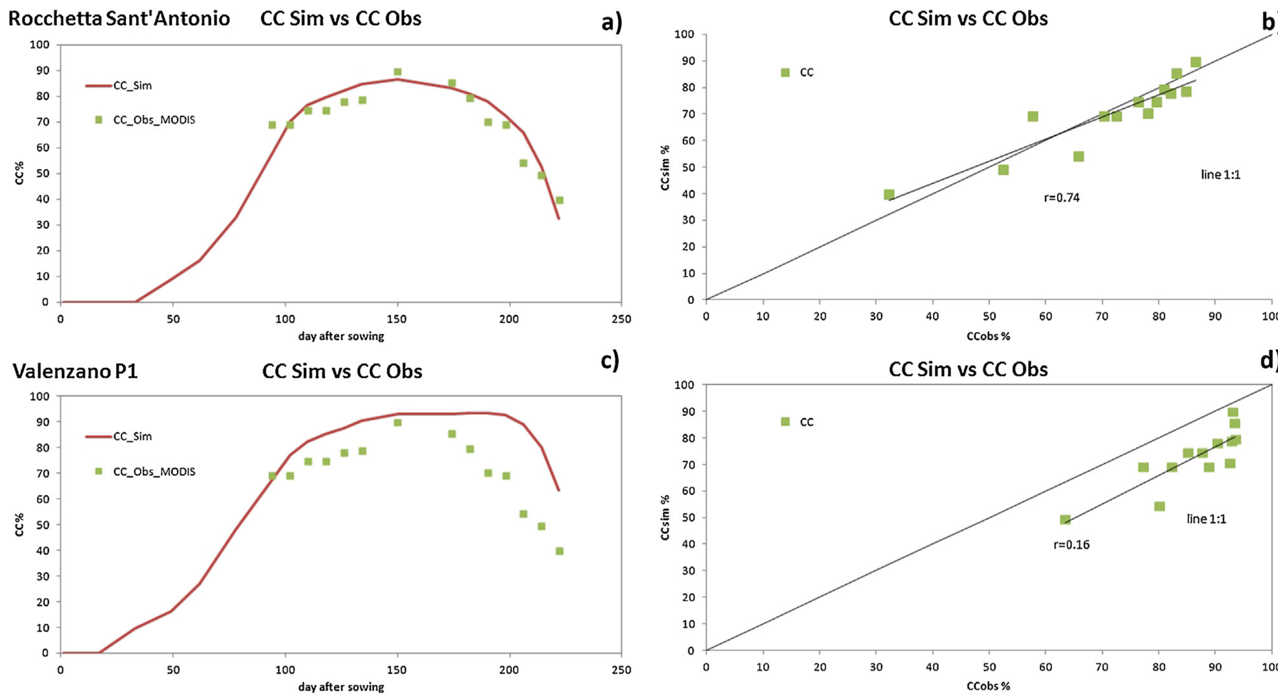

Fig. 11. Comparison between Simulated and Observed CC of winter wheat of Rocchetta Sant'Antonio (a, b) and ValenzanoP1 (c, d) in 2014 (validation).

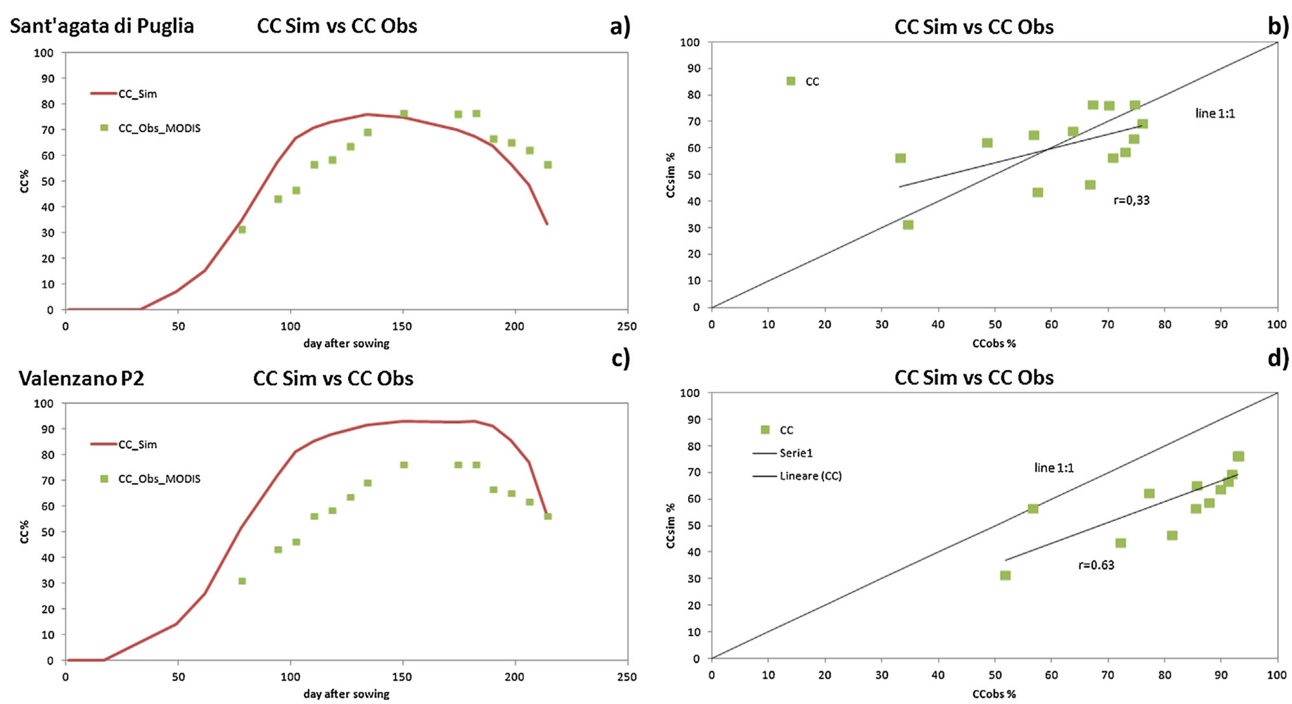

Fig. 12. Comparison between Simulated and Observed CC of winter wheat of Sant'Agata di Puglia (a, b) and ValenzanoP2 (c, d) in 2014 (validation).

tions and the highest trends of CC, which are reflected firstly in B and secondly in Y (Eq. (11), (12):

$$B = K_s \mathrm{WP} \sum \frac{T_r}{\mathrm{ET}_0} \qquad 11$$

$$Y = f_{HI} \mathrm{HI}_0 B \qquad 12$$

where the transpiration T_r is directly proportional to CC development.

4. Conclusions

Remote sensing images are a useful support to model applications, as they allow qualitative and quantitative investigation of objects placed on the earth. In this study the satellite images were used as a support tool for crop phenological cycle calibration. In detail, satellite LAI MODIS data, converted into canopy cover, were compared both in calibration and in validation with AquaCrop model outputs. It is worth mentioning that such comparison involves the use of a relationship between LAI and CC. With

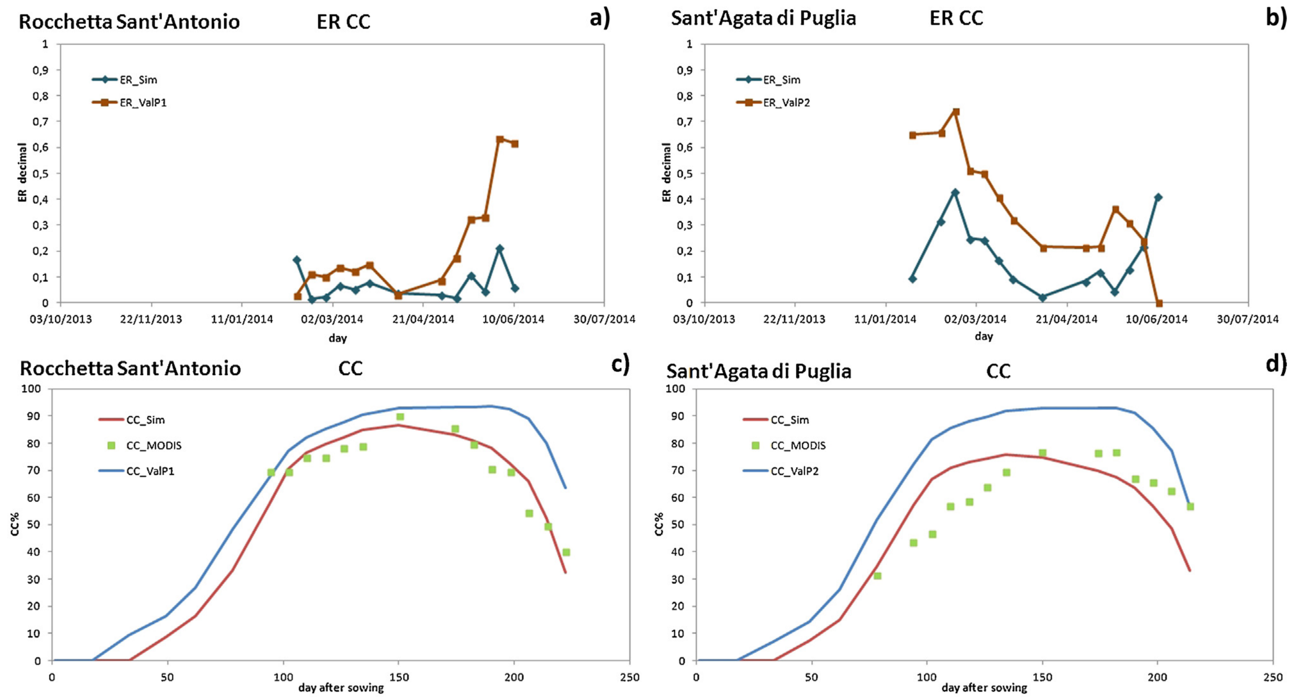

Fig. 13. Simulated, Measured, Valenzano for Rocchetta Sant'Antonio (a) and Sant'Agata di Puglia (b). Comparison of Relative Error in validation between Rocchetta (c) and Sant'Agata (d) with ValenzanoP1 and ValenzanoP2.

this purpose we used an empirical LAI–CC relationship and noticed that few studies are available on this field which deserves further investigation.

The results show that the AquaCrop model gives good estimations of the canopy cover development of winter wheat in two locations in Southern Italy. Remote sensing has provided an important tool to perform calibration, and the convergence of LAI values from high-resolution GeoEye images with the low resolution MODIS images effectively checked the reliability of information obtained by MODIS images.

A local calibration of the parameters within the model, which is possible and made easier by the low number of parameters required in the model, is therefore recommended.

Furthermore a model calibrated based on CC, shows also yield results consistent with real winter wheat productivity in the study area.

Finally, as positive feedback, the use of calibration techniques based on remote sensing may improve the integrated use of models like AquaCrop together with distributed models at basin scale.

Such an integrated approach may lead to important improvements in the evaluation of wheat yield at the regional scale. Also, a combined use of crop growth models with hydrological distributed models could be useful in order to improve the phenomenology description and to obtain acceptable estimates of each hydrologic balance component, such as, for example, a space and temporal variability of soil moisture.

Acknowledgement

This research was funded by Fondazione Cassa di Risparmio di Puglia, Project "Impiego delle immagini da satellite nella gestione della risorsa idrica a scala di bacino", Scientific Coordinator prof. Francesco Gentile, University of Bari.

References

Addiscott, T., Smith, J., Bradbury, N., 1995. Critical evaluation of models and their parameters. J. Environ. Qual. 24, 803–807.

Ahmadi, S.H., Mosallaeepour, E., Kamgar-Haghighi, A.A., Sepaskhah, A.R., 2015. Modeling maize yield and soil water content with AquaCrop under full and deficit irrigation managements. Water Resour. Manage. 29, 2837–2853.

Allen, R.G., Pereira, L.S., Raes, D., Smith, M., 1998. Crop evapotranspiration—guidelines for computing crop water requirements. Irrigation Drainage, 56. FAO, Rome, Italy, pp. 300.

Altobelli, A., Napolitano, R., Bressan, E., Mignozzi, K., Hubina, T., Feoli, E., 2007. Prodotti MODIS per lo studio della vegetazione: teoria, applicazione pratica e problemi di scala, VIII Meeting degli utenti italiani di GRASS, Palermo, 14–16 febbraio 2007.

Andarzian, B., Bannayan, M., Steduto, P., Mazraeh, H., Barati, M., Barati, M., Rahnama, A., 2011. Validation and testing of the AquaCrop model under full and deficit irrigated wheat production in Iran. Agri. Water Manage. 100, 1–8.

Aquilino, M., Novelli, A., Tarantino, E., Iacobellis, V., Gentile, F., 2014. Evaluating the potential of GeoEye data in retrieving LAI at watershed scale. Proceedings of Spie Volume 9239—Remote Sensing for Agriculture, Ecosystems, and Hydrology XVI.

Araya, A., Keesstra, S., Stroosnijder, L., 2010. Simulating yield response to water of Teff (*Eragrostis tef*) with FAO's AquaCrop model. Field Crops Res. 116, 196–204.

Bach, H., Schneider, K., Verhoff, W., Stolz, R., Mauser, W., Van Leeuwen, H., Schouten, L., Borgeaud, M., 2001. Retrieval of geo-and biophysical information from remote sensing through advanced combination of a land surface process model with inversion techniques in the optical and microwave spectral range. Physical Measurements and Signatures in Remote Sensing, International Symposium, 639–647.

Biondi, D., Freni, G., Iacobellis, V., Mascaro, G., Montanari, A., 2012. Validation of hydrological models: conceptual basis, methodological approaches and a proposal for a code of practice. Phys. Chem. Earth 42–44, 70–76, http://dx.doi.org/10.1016/j.pce.2011.07.037.

Buckley, D.S., Isebrands, J.G., Sharik, T.L., 1999. Practical field methods of estimating canopy cover, PAR, and LAI in Michigan oak and pine stands. North. J. Appl. For. 16 (1), 25–32.

Brisson, N., Mary, B., Ripoche, D., Jeuffroy, M.H., Ruget, F., Nicoullaud, B., Gate, P., Devienne-Barret, F., Antonioletti, R., Durr, C., 1998. STICS: a generic model for the simulation of crops and their water and nitrogen balances. I. Theory and parameterization applied to wheat and corn. Agronomie 18, 311–346.

Caliandro, A., Lamaddalena, N., Stelluti, M., Steduto, P., 2005. Caratterizzazione agroecologica della Regione Puglia in funzione della potenzialità produttiva: Progetto Acla 2. Puglia, Bari, Italy, Opuscolo Divulgativo.

Chopping, M., Moisen, G.G., Su, L., Laliberte, A., Rango, A., Martonchik, J.V., Peters, D.P., 2008. Large area mapping of southwestern forest crown cover, canopy height, and biomass using the NASA multiangle imaging spectro-radiometer. Remote Sens. Environ. 112, 2051–2063.

Clevers, J., 1989. Application of a weighted infrared-red vegetation index for estimating leaf area index by correcting for soil moisture. Remote Sens. Environ. 29, 25–37.
Darvishzadeh, R., Skidmore, A., Schlerf, M., Atzberger, C., 2008. Inversion of a radiative transfer model for estimating vegetation LAI and chlorophyll in a heterogeneous grassland. Remote Sens. Environ. 112, 2592–2604.
Dente, L., Satalino, G., Mattia, F., Rinaldi, M., 2008. Assimilation of leaf area index derived from ASAR and MERIS data into CERES–Wheat model to map wheat yield. Remote Sens. Environ. 112, 1395–1407.
Doraiswamy, P., Hatfield, J., Jackson, T., Akhmedov, B., Prueger, J., Stern, A., 2004. Crop condition and yield simulations using Landsat and MODIS. Remote Sens. Environ. 92, 548–559.
Doorenbos, J., Kassam, A.H., 1979. Yield response to water. Irrigation and Drainage, 33. FAO, Rome, Italy, pp. 193.
Fang, H., Liang, S., Hoogenboom, G., Teasdale, J., Cavigelli, M., 2008. Corn-yield estimation through assimilation of remotely sensed data into the CSM–CERES–Maize model. Int. J Remote Sens. 29, 3011–3032.
Fang, H., Liang, S., Hoogenboom, G., 2011. Integration of MODIS LAI and vegetation index products with the CSM–CERES–Maize model for corn yield estimation. Int. J. Remote Sens. 32, 1039–1065.
Fao, 2010. Global forest resources assessment 2010: Main report. Food and Agriculture Organization of the United Nations.
Fei, Y., Jiulin, S., Hongliang, F., Zuofang, Y., Jiahua, Z., Yunqiang, Z., Kaishan, S., Zongming, W., Maogui, H., 2012. Comparison of different methods for corn LAI estimation over northeastern China. Int. J. Appl. Earth Obs. Geoinform. 18, 462–471.
Geerts, S., Raes, D., Garcia, M., Miranda, R., Cusicanqui, J.A., Taboada, C., Mendoza, J., Huanca, R., Mamani, A., Condori, O., Mamani, J., Morales, B., Osco, V., Steduto, P., 2009. Simulating yield response to water of quinoa (Chenopodium quinoa Willd.) with FAO-AquaCrop. Agron. J. 101, 499–508.
Griffin, A.M.R., Popescu, S.C., Zhao, K., 2008. Using LIDAR and normalized difference vegetation index to remotely determine LAI and percent canopy cover. In: Hill, R.A., Rosette, J., Suárez, J. (Eds.), Proceedings of 8th International Conference on LIDAR Applications in Forest Assessment and Inventory. Edinburgh, UK, pp. 446–455.
Gupta, H.V., Kling, H., Yilmaz, K., Martinez, G.F., 2009. Decomposition of the mean squared error and NSE performance criteria: implications for improving hydrological modelling. J. Hydrol. 377 (1–2), 80–91.
Homer, C., Dewitz, J., Fry, J., Coan, M., Hossain, N., Larson, C., Herold, N., McKerrow, A., VanDriel, J.N., Wickham, J., 2007. Completion of the 2001 national land cover database for the counterminous United States. Photogramm. Eng. Remote Sens. 73, 337.
Houborg, R., McCabe, M., Cescatti, A., Gao, F., Schull, M., Gitelson, A., 2015. Joint leaf chlorophyll content and leaf area index retrieval from Landsat data using a regularized model inversion system (REGFLEC). Remote Sens. Environ. 159, 203–221.
Hsiao, T.C., Heng, L., Steduto, P., Rojas-Lara, B., Raes, D., Fereres, E., 2009. AquaCrop—the FAO crop model to simulate yield response to water: III: Parameterization and testing for maize. Agron. J. 101 (3), 448–459.
Hsiao, T.C., Fereres, E., Steduto, P., Raes, D., 2012. Chapter 3.3 AquaCrop parameterization, calibration, and validation guide in Crop Yield Response to Water. Irrigation and Drainage Paper No.66. FAO, Rome, Italy, Steduto, P., Hsiao, T.C., Fereres, E., Raes, D., (Eds.).
Huang, J., Tian, L., Liang, S., Ma, H., Becker-Reshef, I., Huang, Y., Su, W., Zhang, X., Zhu, D., Wu, W., 2015. Improving winter wheat yield estimation by assimilation of the leaf area index from Landsat TM and MODIS data into the WOFOST model. Agric. For. Meteorol. 204, 106–121.
Iacobellis, V., Gioia, A., Milella, P., Satalino, G., Balenzano, A., Mattia, F., 2013. Inter-comparison of hydrological model simulations with time series of SAR-derived soil moisture maps. Eur. J. Remote Sens. 46 (1), 739–757.
Jonckheere, I., Fleck, S., Nackaerts, K., Muys, B., Coppin, P., Weiss, M., Baret, F., 2004. Review of methods for in situ leaf area index determination Part I. Theories, sensors and hemispherical photography. J. Agric. For. Meteorol. 121, 19–35.
Jongschaap, R.E., 2006. Run-time calibration of simulation models by integrating remote sensing estimates of leaf area index and canopy nitrogen. Eur. J. Agron. 24, 316–324.
Kamaludin, H., Lihan, T., Ali Rahman, Z., Mustapha, M.A., Idris, W.M.R., Rahim, S.A., 2013. Integration of remote sensing, RUSLE and GIS to model potential soil loss and sediment yield (SY). Hydrol. Earth Syst. Sci. Discuss 10, 4567–4596.
Knyazikhin, Y., Martonchik, J.V., Myneni, R.B., Diner, D.J., Running, S.W., 1998. Synergistic algorithm for estimating vegetation canopy leaf area index and fraction of absorbed photosynthetically active radiation from MODIS and MISR data. J. Geophys. Resour. 103, 32257–32275.
Kuusk, A., 1998. Monitoring of vegetation parameters on large areas by the inversion of a canopy reflectance model. Int. J. Remote Sens. 19, 2893–2905.
Legates, D.R., McCabe, G.J., 1999. Evaluating the use of goodness-of-fit measures in hydrologic and hydroclimatic model validation. Water Resour. Res. 35, 233–241.
Leuschner, C.H., Voß, S., Foetzki, A., Clases, Y., 2006. Variation in leaf area index and stand leaf mass of European beech across gradients of soil acidity and precipitation. Plant Ecol. 182, 247–258.
Maas, S.J., 1993. Within-season calibration of modeled wheat growth using remote sensing and field sampling. Agron. J. 85, 669–672.
Manfreda, S., Fiorentino, M., Iacobellis, V., 2005. DREAM: a distributed model for runoff, evapotranspiration, and antecedent soil moisture simulation. Adv. Geosci. 2, 31–39.
Milella, P., Bisantino, T., Gentile, F., Iacobellis, V., Trisorio Liuzzi, G., 2012. Diagnostic analysis of distributed input and parameter datasets in Mediterranean basin streamflow modeling. J. Hydrol. 472–473, 262–276.
Mo, X., Liu, S., Lin, Z., Xu, Y., Xiang, Y., McVicar, T., 2005. Prediction of crop yield, water consumption and water use efficiency with a SVAT-crop growth model using remotely sensed data on the North China Plain. Ecol. Model. 183, 301–322.
Moussa, R., Chahinian, N., Bocquillon, C., 2007. Distributed hydrological modeling of a Mediterranean mountainous catchment—model construction and multi-site validation. J. Hydrol. 337, 35–51.
Nain, A.S., Kersebaum, K.Ch., et al., 2007. Calibration and validation of CERES-wheat model for simulating water and nutrients in Germany. In: Kersebaum, K.Ch. (Ed.), Modeling Water and Nutrient Dynamics in Soil? Crop Systems. Springer, 161-181.
Nielsen, D., Miceli-Garcia, J.J., Lyon, J.D., 2012. Canopy cover and leaf area index relationships for wheat, triticale, and corn. Agron. J. 104, 1569–1573.
Nilson, T., Kuusk, A., 2004. Improved algorithm for estimating canopy indices from gap fraction data in forest canopies. Agric. For. Meteorol. 124 (3), 157–169.
Ozdemir, I., 2014. Linear transformation to minimize the effects of variability in understory to estimate percent tree canopy cover using RapidEye data. GISci. Remote Sens. 51, 288–300.
Quaranta, F., Belocchi, A., Fornara, M., Ripa, C., D'Egidio, M. G., 2015. Le varietà di frumento duro in Italia—Risultati della rete nazionale di sperimentazione 1999-2012. Editor: Consiglio per la Ricerca e la Sperimentazione in Agricoltura, Rome—Italy, ISBN: 978-88-97081-31-9.
Raes, D., Steduto, P., Hsiao, T.C., Fereres, E., 2009. AquaCrop—the FAO crop model to simulate yield response to water: II. Main algorithms and software description. Agron. J. 101 (3), 438–447.
Raes, D., Steduto, P., Hsiao, T.C., Fereres, E., 2012. Reference Manual AquaCrop Version 4.0 FAO. Land and Water Division Rome, Italy.
Rinaldi, M., Castrignanò, A., De Benedetto, D., Sollitto, D., Ruggieri, S., Garofalo, P., Santoro, F., Figorito, B., Gualano, S., Tamborrino, R., 2015. Discrimination of tomato plants under different irrigation regimes: analysis of hyperspectral sensor data. Environmetrics 26 (2), 77–88.
Ross, J., 1981. The Radiation Regime and the Architecture of Plant Stands, Dr. W. Junk Publishers, The Hague-Boston-London, 381 pp.
Rouse, J. W., Haas, R. H., Deering, D. W. Schell, J. A., Harlan, J.C., 1974. Monitoring the vernal advancement and retrogradation (Green wave effect) of natural vegetation. NASA/GSFC Type III Final Report, Greenbelt, MD, USA.
Salazar, O., Wesstrom, I., Youssef, M.A., Skaggs, R.W., Joel, A., 2009. Evaluation of the DRAINMOD-N II model for predicting nitrogen losses in loamy sand under cultivation in southeast Sweden. Agric. Water Manage. 96 (2), 267–281.
Saxton, K.E., Rawls, W.J., Romberger, J.S., Papendick, R.I., 1986. Estimating generalized soil–water characteristics from texture. Soil Sci. Soc. Am. J. 50, 1031–1036.
Saxton, K.E., Rawls, W.J., 2006. Soil water characteristic estimates by texture and organic matter for hydrologic solutions. Soil Sci. Soc. Am. J. 70, 1569–1578.
Schneider, K., Mauser, W., 2001. Using remote sensing data to model water, carbon, and nitrogen fluxes with PROMET-V. Europto Remote Sensing. International Society for Optics and Photonics, 12–23.
Semaika, M., Rady, A.H., 1987. Factors affecting crop coefficient when calculating crop evapotranspiration, irrigation and water allocation. Proceedings of the Vancouver Symposium, IAHS Publ. No. 169.
Steduto, P., Hsiao, T.C., Raes, D., Fereres, E., 2009. AquaCrop—the FAO crop model to simulate yield response to water: I: concepts and underlying principles. Agron. J. 101, 426–437.
Steduto, P., Raes, D., Hsiao, T.C., Fereres, E., Heng, L., Izzi, G., Hoogeveen, J., 2008. AquaCrop: a new model for crop prediction under water deficit conditions. Options Méditerr. Ser. A 80.
Stenberg, P., Rautiainen, M., Manninen, T., Voipio, P., Smolander, H., 2004. Reduced simple ratio better than NDVI for estimating LAI in Finnish pine and spruce stands. Silva Fennica 38, 3–14.
Tarantino, E., Novelli, A., Laterza, M., Gioia, A., 2015a. Testing high spatial resolution WorldView-2 imagery for retrieving the leaf area index. Third International Conference on Remote Sensing and Geoinformation of the Environment. International Society for Optics and Photonics, pp. 95351N-95351N-95358.
Tarantino, E., Novelli, A., Laterza, M., Gioia, A., 2015b. Testing high spatial resolution WorldView-2 imagery for retrieving the leaf area index. Third International Conference on Remote Sensing and Geoinformation of the Environment International Society for Optics and Photonics (pp. 95351N-95351N).
Ungaro, F., Calzolari, C., 2001. Using existing soil databases for estimating retention properties for soils of the Pianura Padano-Veneta region of North Italy. Geoderma 99, 99–121.
Van Dam, J., Huygen, J., Wesseling, J., Feddes, R., Kabat, P., Van Walsum, P., Groenendijk, P., Van Diepen, C., 1997. Theory of SWAP version 2.0. Technical Document 45, 167.
van der Knijff, J.M., Jones, R.J.A., Montanarella, L., 2000. Soil Erosion Risk Assessment in Europe European Commission Directorate General JRC, Joint Research Centre, Space Applications Institute, European Soil Bureau.
Verhoef, W., 1984. Light scattering by leaf layers with application to canopy reflectance modeling: the SAIL model. Remote Sens. Environ. 16, 125–141.
Wang, Q., Adiku, S., Tenhunen, J., Granier, A., 2005. On the relationship of NDVI with leaf area index in a deciduous forest site. Remote Sens. Environ. 94 (2), 244–255.

Weiss, M., Baret, F., Myneni, R.B., Pragnère, A., Knyazikhin, Y., 2000. Investigation of a model inversion technique to estimate canopy biophysical variables from spectral and directional reflectance data. Agronomie 20, 3–22.

Weiss, M., Troufleau, D., Baret, F., Chauki, H., Prévot, L., Olioso, A., Bruguier, N., Brisson, N., 2001. Coupling canopy functioning and radiative transfer models for remote sensing data assimilation. Agric. For. Meteorol. 108, 113–128.

Xiong, X., Barnes, W., 2006. An overview of MODIS radiometric calibration and characterization. Adv. Atmos. Sci. 23, 69–79.

Xu, W., Jiang, H., Huang, J., 2011. Regional crop yield assessment by combination of a crop growth model and phenology information derived from MODIS. Sens. Lett. 9, 981–989.

Zheng, G., Moskal, L.M., 2009. Retrieving leaf area index (LAI) using remote sensing: theories, methods and sensors. Sensors 9, 2719–2745.

Further reading

Allen, R.G., Pruitt, W.O., Wright, J.L., Howell, T.A., Ventura, F., Snyder, R., Itenfisu, D., Steduto, P., Berengena, J., Yrisarry, J.B., Smith, M., Pereira, L.S., Raes, D., Perrier, A., Alves, I., Walter, I., Elliott, R., 2006. A recommendation on standardized surface resistance for hourly calculation of reference ETo by the FAO56 Penman–Monteith method. Agric. Water Manage. 81, 1–22.

Carreiras, J.M., Pereira, J.M., Pereira, J.S., 2006. Estimation of tree canopy cover inevergreen oak woodlands using remote sensing. For. Ecol. Manage. 223, 45–53.

Coulston, J.W., Jacobs, D.M., King, C.R., Elmore, I.C., 2013. The influence of multi-season imagery on models of canopy cover. Photogramm. Eng. Remote Sens. 79, 469–477.

Erfanifard, Y., Khodaei, Z., Shamsi, R.F., 2014. A robust approach to generate canopy cover maps using UltraCam-D derived orthoimagery classified by support vector machines in Zagros woodlands, West Iran. Eur. J. Remote Sens. 47, 773–792.

Klemeš, V., 1986. Operational testing of hydrological simulation models. Hydrol. Sci. J. 31, 13–24.

Jones, J.W., Hoogenboom, G., Porter, C.H., Boote, K.J., Batchelor, W.D., Hunt, L.,Wilkens, P.W., Singh, U., Gijsman, A.J., Ritchie, J.T., 2003. The DSSAT cropping system model. Eur. J. Agron. 18, 235–265.

Knyazikhin, Y., Glassy, J., Privette, J.L., Tian, Y., Lotsch, A., Zhang, Y., Wang, Y., Morisette, J.T., Votava, P., Myneni, R.B., Nemani, R.R., Running, S.W., 1999. MODIS Leaf Area Index (LAI) and Fraction of Photosynthetically Active Radiation Absorbed by Vegetation (FPAR) Product (MOD15) Algorithm, Theoretical Basis Document. NASA Goddard Space Flight Center, Greenbelt, MD 20771, USA.

Korhonen, L., Korhonen, K.T., Rautiainen, M., Stenberg, P., 2006. Estimation offorest canopy cover: a comparison of field measurement techniques. Silva Fennica 40, 577.

Penman, H.L., 1948. Natural evaporation from open water, bare soil, and grass. Proc. R. Soc. Lond., Ser. A 193, 120–145.

Samani Majd, A.M., Bleiweiss, M.P., DuBois, D., Shukla, M.K., 2013. Estimation of the fractional canopy cover of pecan orchards using Landsat 5 satellite data, aerial imagery, and orchard floor photographs. Int. J. Remote Sens. 34, 5937–5952.

Tabari, H., Grismer, M.E., Trajkovic, S., 2013. Comparative analysis of 31 reference evapotranspiration methods under humid conditions. Irrig. Sci. 31, 107–117.

Williams, M.S., Patterson, P.L., Mowrer, H.T., 2003. Comparison of ground sampling methods for estimating canopy cover. For. Sci. 49, 235–246.